Synthesis, structures, and magnetic properties of crystals of dinuclear copper(II) and cobalt(II) complexes with 3-(3,5-dimethylpyrazol-1-yl)-6-R-1,2,4,5-tetrazines

E. V. Cherdantseva,[a] D. V. Starichenko,[b] P. A. Slepukhin,[c] R. I. Ishmetova,[c] Yu. N. Shvachko,[b] A. V. Korolev,[b] G. L. Rusinov,[c] V. V. Ustinov,[b] A. I. Matern,[a] and V. N. Charushin[c]*

[a]*B. N. Yeltsin Ural State Technical University, Bldg. 3, 19 ul. Mira, 620002 Ekaterinburg, Russian Federation*
[b]*Institute of Metal Physics, Ural Branch of the Russian Academy of Sciences, 18 ul. S. Kovalevskoy, 620041 Ekaterinburg, Russian Federation*
[c]*I. Ya. Postovskii Institute of Organic Synthesis, Ural Branch of the Russian Academy of Sciences, 22/20 ul. S. Kovalevskoy/Akademicheskaya, 620041 Ekaterinburg, Russian Federation*
Fax: + 7 (343) 374 1189. E-mail: rusinov@ios.uran.ru

Dinuclear complexes of Cu^{II} with 3-(3,5-dimethylpyrazol-1-yl)-6-(2-hydroxyethylamino)-1,2,4,5-tetrazine (**1**) and Co^{II} with 3-(3,5-dimethylpyrazol-1-yl)-6-(piperidin-1-yl)-1,2,4,5- tetrazine (**2**) were synthesized and structurally characterized, and the magnetic (SQUID) and resonance (EPR) properties of van der Waals crystals based on these complexes were studied. Unusual behavior of the effective magnetic moment $\mu_{eff}(T)$ is observed at $T < 60$ K. A nonmonotonic increase in $\mu_{eff}(T)$ for **1** (~6 %) and a 20% reduction of $\mu_{eff}(T)$ for **2** have a common origin and are due to the influence of spin-orbital coupling on the character of the splitting between the t_{2g} and e_g levels of the central ion. Distortions of the coordination site "switch on" a positive (**1**) or negative (**2**) contribution of the orbital magnetic moment near 6 K. Irreversible temperature behavior of $\mu_{eff}(T)$ in the heating and cooling regimes in the vicinity of 60 K suggests that the character of structural distortions and the magnetic properties are related to ligand geometry. This factor plays a significant role in crystal engineering of magnetoactive structures with polynitrogen ligands.

Key words: dinuclear complexes, 3-(3,5-dimethylpyrazol-1-yl)-6-R-1,2,4,5-tetrazines, X-ray analysis, EPR spectroscopy, SQUID magnetometry, spin magnetism.

Design of polyfunctional magneto-active materials and molecular magnetics based on paramagnetic complexes has become one of the most rapidly developing fields of interdisciplinary research involving modern chemical science and physics of magnetic phenomena.[1] Polynitrogen heterocycles are promising molecular spacers between paramagnetic metal ions for the assembly of high-spin blocks. In particular, of interest are polydentate tetrazine ligands where the coordination site geometry can be controlled by electronic and steric effects; this is the reason for the search for tunable spin transitions (crossovers) in the metal-chelate structures based on them. 3,6-Bis(3,5-dimethylpyrazol-1-yl)-1,2,4,5-tetrazine and its derivatives are promising ligands.[2—5] In the present work, taking isolated dimeric structures as examples, we have shown that structural distortions in the coordination site cause significant changes in the magnitude of the effective magnetic moment even in the absence of exchange interactions between the 3d-metal (Cu^{II} and Co^{II}) ions.

Results and Discussion

The reactions of Cu^{II} chloride with 3-(3,5-dimethylpyrazol-1-yl)-6-(2-hydroxyethylamino)-1,2,4,5-tetrazine and Co^{II} chloride with 3-(3,5-dimethylpyrazol-1-yl)-6-piperidino-1,2,4,5-tetrazine in acetonitrile on heating resulted in crystalline complexes **1** and **2**, respectively (Schemes 1 and 2).

The structures of the complexes (Figs 1 and 2) were proved by elemental analysis, IR spectroscopy, and X-ray diffraction analysis. The IR spectra of complexes **1** and **2** in the absorption regions of the 3,6-dimethylpyrazole substituent and tetrazine ring are significantly different from those of the starting tetrazines; this confirms the conclusion that both fragments are involved in the coordination to the metal atoms.[6] Indeed, in both cases X-ray studies revealed the formation of chlorine-bridged dinuclear complexes in which ligands form coordination bonds involving the pyrazole and tetrazine ring nitrogen atoms. In com-

Published in Russian in *Izvestiya Akademii Nauk. Seriya Khimicheskaya,* No. 4, pp. 703—709, April, 2010.
1066-5285/10/5904-0717 © 2010 Springer Science+Business Media, Inc.

Scheme 1

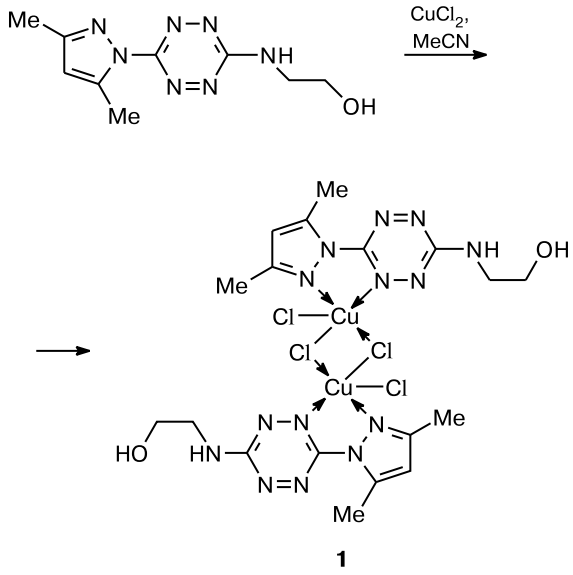

1

Scheme 2

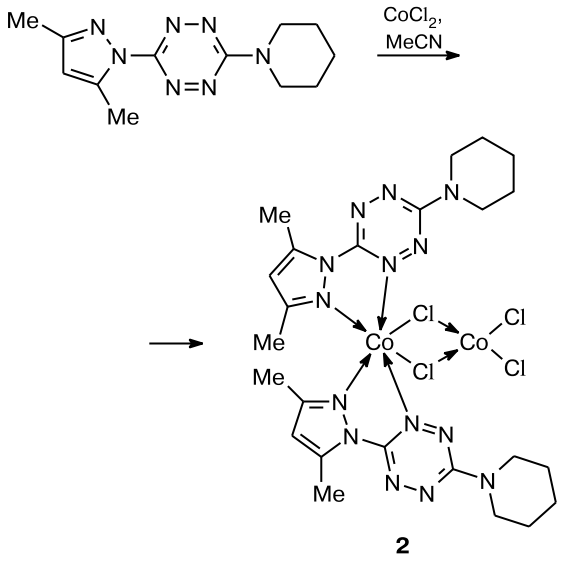

2

plex **1**, both copper atoms are five-coordinate, two chlorine atoms are bridging, and the ethanolamino fragment of the ligand is not involved in complexation (see Fig. 1). In complex **2**, each cobalt atom has its own environment with different stereometry (see Fig. 2). In particular, the cobalt atom bound to the tetrazine ligand is six-coordinate (the coordination polyhedron is a distorted octahedron), while the Co atom bound to the chlorine atoms is four-coordinate (the coordination polyhedron is a distorted tetrahedron).

The magnetic and resonance properties of complexes **1** and **2** were studied. In structure **1** (Table 1), both copper

Table 1. Selected bond lengths (d) and bond angles (ω) in complexes **1** and **2** determined by X-ray analysis

Bond length	d/Å	Angle	ω/deg
		Complex **1**	
Cu(1)—N(6)	1.998(3)	Cu(1)—Cl(2)—Cu(1)$^{\#1}$	90.61(3)
Cl(2)—Cu(1)$^{\#1}$	2.6109(10)	Cl(1)—Cu(1)—Cl(2)$^{\#1}$	109.65(4)
Cu(1)—Cl(2)	2.2538(9)	N(6)—Cu(1)—N(1)	79.01(11)
Cu(1)—N(1)	2.047(3)	N(1)—Cu(1)—Cl(1)	148.13(8)
Cu(1)—Cl(1)	2.2442(9)	N(6)—Cu(1)—Cl(2)	171.54(8)
		Complex **2**	
Co(1)—N(6)	2.119(2)	N(1)$^{\#1}$—Co(1)—Cl(1)	177.06(7)
Co(1)—N(1)	2.152(2)	N(1)—Co(1)—Cl(1)	88.99(6)
Co(2)—Cl(1)	2.3232(8)	Cl(1)—Co(2)—Cl(1)$^{\#1}$	94.05(4)
Co(1)—Cl(1)	2.4357(8)	N(6)$^{\#1}$—Co(1)—N(6)	157.32(13)
Co(2)—Cl(2)	2.2225(11)	Co(2)—Cl(1)—Co(1)	88.72(3)

Symmetry transformations: $^{\#1}$ $-x+2, -y+2, z$.

atoms of the dinuclear complex are separated from the corresponding atoms in adjacent dimers by so long distances (>6.5 Å) that exchange interactions between them can be ignored (see Table 1). The magnetic behavior of this compound is determined by the properties of the isolated centrosymmetric dimer. Both copper atoms are in distorted square-pyramidal coordination environment (with the N(1)—N(6)—Cl(1)—Cl(2) base and the Cl(2) $[1-x, -y, 1-z]$ vertex).

The temperature dependence of the static magnetic susceptibility $\chi(T)$ was measured as the temperature dependence of the effective magnetic moment $\mu_{eff}(T)$ according to the relationship $\mu_{eff} \sim (\chi T)^{1/2}$. The results obtained (Fig. 3) suggest no magnetic interactions between the unpaired electrons in copper ions up to 60 K. Since at 293 K atoms in the dimer are structurally equivalent, the value $\mu_{eff} = 2.58\ \mu_B$ corresponds to an effective moment of 1.82 μ_B per Cu atom. This is somewhat larger than the theoretical value (1.73 μ_B) for the spin $S = 1/2$, but falls near the range of experimental μ_{eff} values of the noninteracting Cu^{II} spins (1.8—2.2 μ_B) taking into account the g-factor values measured by EPR spectroscopy (see below). In the temperature range 2 K < T < 60 K, the temperature dependence exhibits a well-defined maximum at 5.8 K; at this point μ_{eff} reaches a value of 2.74 μ_B (1.94 μ_B per Cu atom). The magnitude and position of the maximum are independent of external magnetic field (0.5—1.0 T) and on the regime of SQUID measurements (heating or cooling). This excludes the "texturing" of polycrystals in the magnetic field and a nonmonotonic decrease in the contribution of the diamagnetic molecular framework. The nonmonotonic behavior of $\mu_{eff}(T)$ does not obey the Bleaney—Bowers equation for dimers with pairs of spins $S = 1/2$.

The magnetic field dependence of the magnetization $M(B)$ measured at $T = 2$ K is correctly described by the

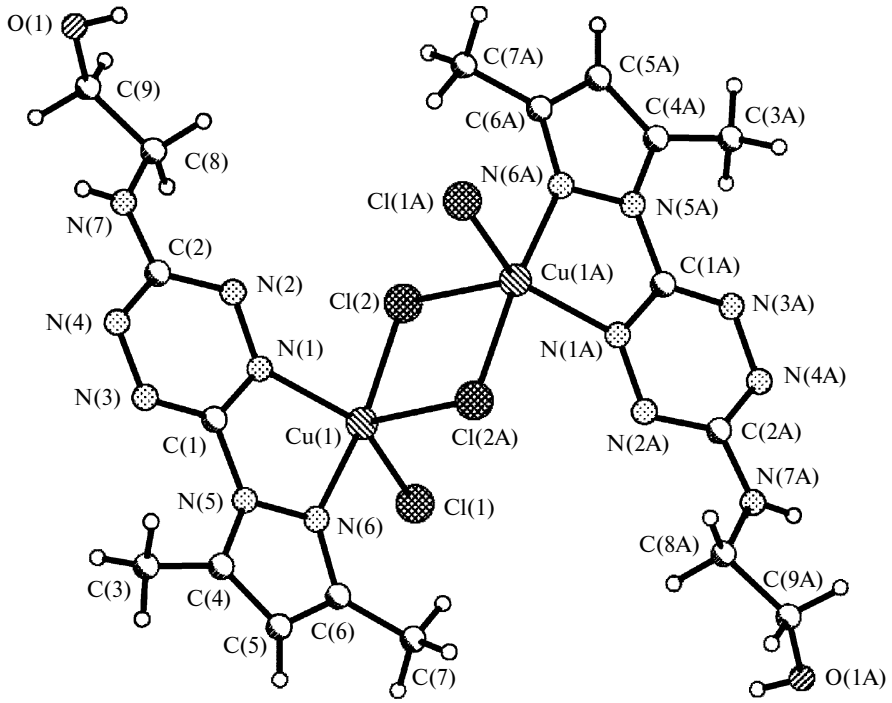

Fig. 1. General view of complex **1** ("A" denotes symmetrically equivalent atoms).

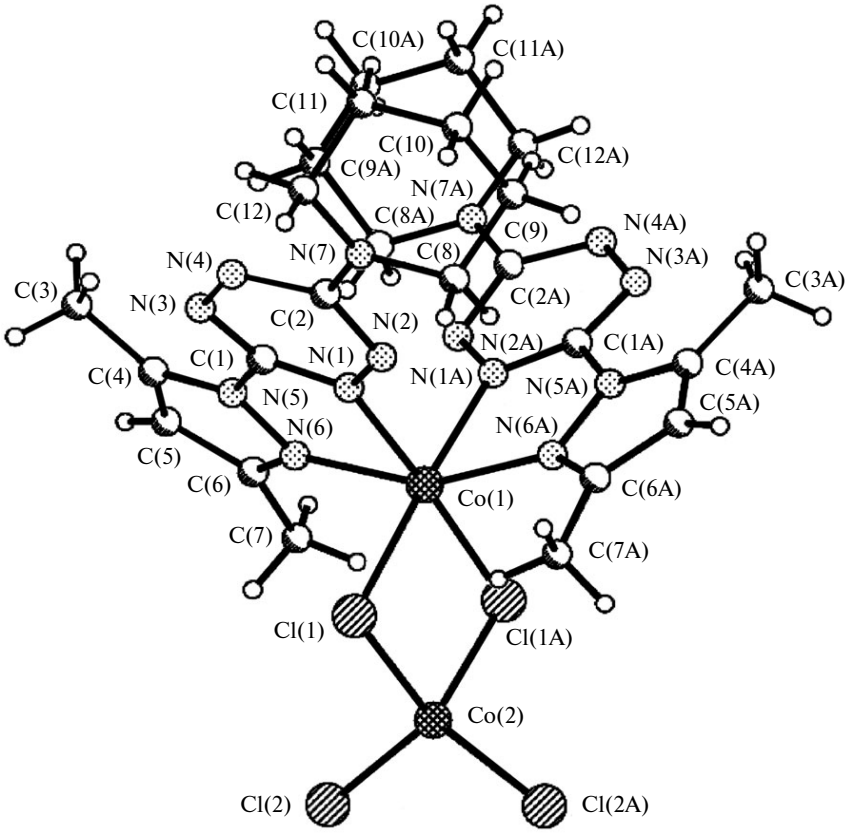

Fig. 2. General view of complex **2** ("A" denotes symmetrically equivalent atoms).

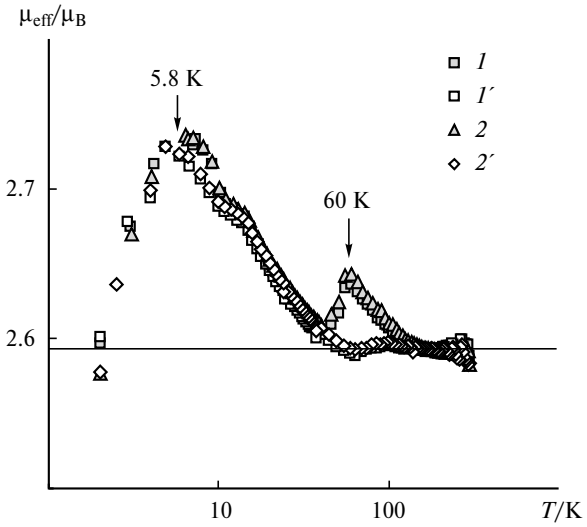

Fig. 3. Temperature dependence of the effective magnetic moment (μ_{eff}) of complex **1** measured at B = 0.5 (*1*, *1′*) and 1.0 T (*2*, *2′*) in the heating (*1*, *2*) and cooling (*1′*, *2′*) regimes. Temperature is given in the logarithmic scale.

Brillouin function for two noninteracting spins $S = 1/2$ (Fig. 4). Since at the outermost points of the temperature interval 2 K < T < 60 K the spins in the dimer behave as noninteracting, the nonmonotonic increase in μ_{eff} within this temperature interval can not be due to ferromagnetic correlations. The irreversible character of the $\mu_{eff}(T)$ dependence near 60 K is also unexpected. When measurements are carried out in the heating regime (temperature increases from 2 to 300 K), the second maximum is observed, although measurements in the cooling regime show no maximum (see Fig. 3). This feature is magnetic field-independent and has no effect on the low-temperature maximum.

The EPR spectra of complex **1** exhibit a symmetric singlet line with ΔB(293 K) = 40 G; the g_2 and g_3 components of the anisotropic g-factor and the hyperfine structure from the nuclear spins of N(1) and N(6) are not observed, so one has g(293 K) = 2.214. At high temperatures, one has ΔB(393 K) = 57 G and g = 2.174. As the temperature decreases to 170 K, ΔB monotonically decreases to 34 G (Fig. 5) and then becomes temperature-independent; this is a characteristic feature of effective line narrowing, g(93 K) = 2.213. In the line narrowing region, the g-factor is also temperature-independent. The normalized integrated intensity of the EPR signal $I(T)/I$(90 K) determined according to Schumacher—Slichter technique considerably increases in the effective narrowing region and one gets I(170 K)/I(293 K) = 3. In the temperature range where the narrowed signal is observed (90 K < T < 170 K) the temperature behavior of the integrated intensity of the EPR signal obeys the Curie law. Figure 5 presents the temperature behavior of the inverse of integrated intensity, $[I(T)/I(90\ K)]^{-1}$; the corresponding theoretical Curie plot is shown by the solid straight line.

Changes in μ_{eff} at low temperatures can not be attributed to thermally activated motions of molecular groups because the corresponding energy ($\Delta E_a/\kappa \approx 6$ K) is inconsistent with the energies of stretching and/or torsional vibrations of symmetrical and nonsymmetrical tetrazine derivatives. The main absorption bands selected from a large array of Raman and IR spectral data lie in the regions 1276—1050, 970—942 ("breathing"), and 758—472 cm^{-1} (deformation).[6] However, the irreversible character of the magnetic response at 60 K is a characteristic feature of just the configurational instability of the coordination environment. At room temperature, the square base of the pyramid is shrinked along the N(1)—N(6) side (N(1)—Cu(1)—N(6) angle is about 80°) and the central ion is slightly shifted (by about 6%) toward this

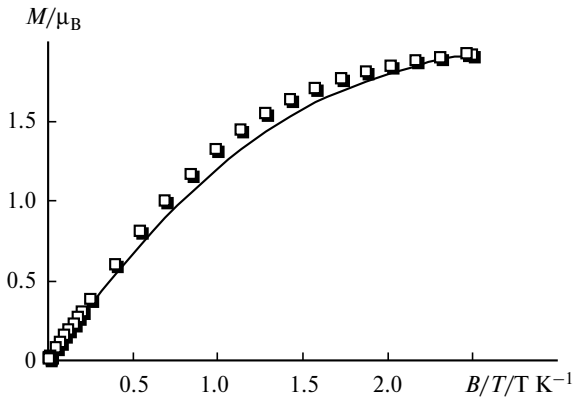

Fig. 4. Magnetic field dependence of the magnetization of complex **1** at T = 2 K: open squares are experimental data and the solid line denotes the Brillouin dependence for two noninteracting spins, $S = 1/2 + 1/2$, in the dimer.

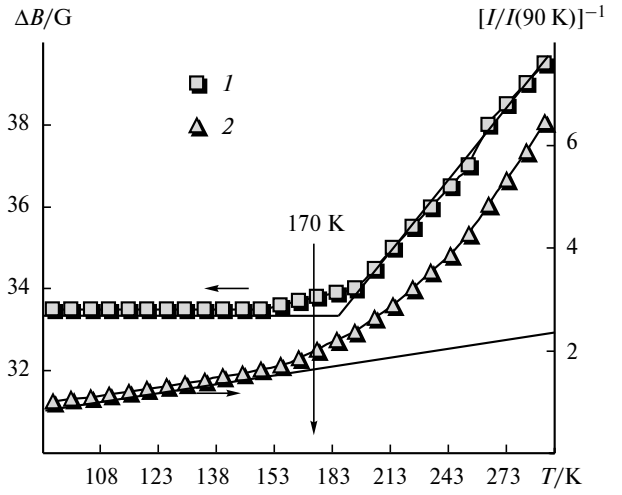

Fig. 5. Temperature dependence of EPR linewidth ΔB (*1*) and the inverse integrated intensity of EPR signal $[I(T)/I(90\ K)]^{-1}$ (*2*) for the copper complex **1**. The straight lines at T < 170 K denote correlations between the effectively narrowed EPR signal and the Curie-type dependence for $I(T)$.

side. The Cl(1) atom deviates from the N(1)—Cu(1)—N(6) basal plane, so the N(1)—Cu(1)—Cl(1) angle is 148° (see Table 1). Despite significant distortions and weakness of the ligand field in the spectrochemical series (3 Cl^-), the upper energy level corresponds to the $d_{x^2-y^2}$ ($l = 2$) orbital (e_g symmetry type) and is orbitally nondegenerate. Note that the contribution of the orbital moment can increase the value $\mu^2_{eff} = [4S(S + 1) + L(L + 1)]$ per Cu^{II} atom to 3 μ_B ($l = 2$). However, partial "unfreezing" of the orbital moment provides no explanation for the increase in μ_{eff}, because for the e_g-levels the orbital moment is always totally "frozen". At the same time, when considering the distorted site of the weak-field ligand, one should take into account the spin-orbital coupling, so that the complete energy diagram has a multiplicity of $(2S + 1)(2L + 1)$ and becomes dependent on the extent of structural distortions.[7] The type of the ground state is determined by the balance between the energy of structural distortions of the coordination site and the spin-orbital coupling energy $\sim\lambda S$.[8] Assume that at $T = 6$ K the partial magnetic responses from Cu(1) and Cu(2) are different; then, one has $\mu_{eff}^{exp} = 2.74\ \mu_B$, which is close to $\mu_{eff}^{calc} = 2.83\ \mu_B$, where one copper atom is characterized by the orbital contribution $l_{eff} = 1$. A more detailed description of the mechanism in question for this complex requires low-temperature structural studies and quantum chemical calculations. However, in any case the most probable explanation for the nonmonotonic increase in the magnetic moment consists in switching on the orbital magnetic contribution through a subtle change in the configuration of the coordination environment upon temperature-induced contraction of the crystal. Here, a significant role is played by the pyrazolyl-tetrazine framework of the ligand.

In structure **2**, the distances between the cobalt atoms of neighboring dinuclear complexes are also too long (>9.5 Å) to give rise to long-range magnetic ordering at $T > 2$ K. At the same time, one could expect that specific features of the ligand shell will manifest themselves in magnetic properties in the same temperature interval as for complex **1**. However, since in this structure the Co(1) and Co(2) atoms are initially in different coordination environment, the temperature dependences of the magnetic characteristics are also qualitatively different.

The fact that complex **2** exhibits no c.w. EPR signal in the X-band at 77—300 K indirectly indicates a high-spin state ($S = 3/2$) of both atoms in which, unlike the low-spin state ($S = 1/2$), the Co^{II} ions are characterized by very short relaxation times and their EPR spectra can only be observed at $T \leq 15$ K.[9]

The $\mu_{eff}(T)$ dependences for complex **2** measured in the magnetic fields $B = 0.5$ and 1.0 T in the heating and cooling regimes are shown in Fig. 6. In the temperature range 60—300 K, one has $\mu_{eff} = 6.22\ \mu_B$ irrespective of the B value and measurement regime. On cooling below 60 K, μ_{eff} monotonically decreases to 5.60 μ_B (0.5 T) and 4.97 μ_B (1.0 T). As for complex **1**, a region of irreversible behavior of μ_{eff}, which is not produced by antiferromagnetic interactions within the dimer, is detected for structure **2** near $T = 60$ K. The observed dependences are not described by the van Vleck temperature functions. The μ_{eff} values are observed at $\kappa T/|\lambda| < 1$ on all doubly charged t_{2g}-ions provided that the spin-orbital coupling is "switched on". Transition of a particular complex to the low-spin state ($S = 1/2$) with $\mu_{eff} = 1.73\ \mu_B$ (spin crossover) can erroneously be treated as an indication of antiferromagnetic superexchange in the structure. The effective magnetic moment of Co^{II} in the high-spin state can also vary from 3.87 to 5.2 μ_B because the contribution of the orbital moment depends on the character of the splitting of the t_{2g}-level.

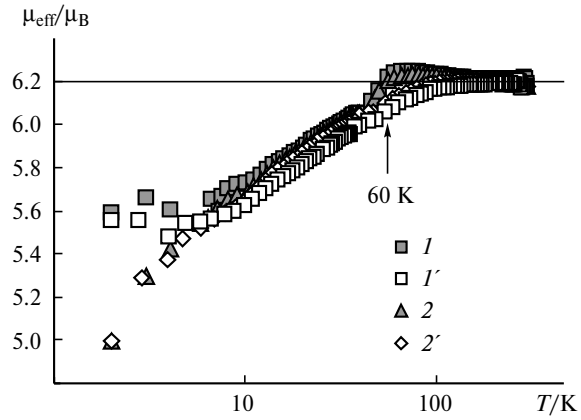

Fig. 6. Temperature dependence of the effective magnetic moment $\mu_{eff}(T)$ of complex **2** measured at $B = 0.5$ T (*1*, *1′*) and 1.0 T (*2*, *2′*) in the heating (*1*, *2*) and cooling (*1′*, *2′*) regimes. Temperature is given in the logarithmic scale.

In complex **2**, the cobalt ions are in different coordination environment, *viz.*, the coordination polyhedron is a distorted octahedron for Co(1) and a tetrahedron for Co(2). The theoretical value of μ_{eff} for the Co(2) ion in the tetrahedral environment $\mu_{eff}^{calc} = 3.87\ \mu_B$ corresponds to the maximum spin moment of the t_{2g}-level ($S = 3/2$). The symmetry of the environment of Co(2) is conserved even at as low temperature as about 2 K; therefore, the spin state of Co(2) is also temperature-independent.

The following additive relationship is valid for a complex containing two types of noninteracting paramagnetic centers: $\mu^2_{eff} = \mu^2(1) + \mu^2(2)$. The contribution of the paramagnetic centers 1 and 2 can vary depending on the spin state and/or temperature. Taking into account the experimental value (6.22 μ_B) and the theoretical estimate (3.87 μ_B) for the contribution of the Co(2) ion, for the Co(1) ion one gets $\mu_{eff}(1) = 4.87\ \mu_B$ at $T > 60$ K; this is close to a value of 5.2 μ_B ($\mu_{eff}^{calc}(300\ K) = 6.48\ \mu_B$). For the smallest experimental value $\mu_{eff} = 4.97\ \mu_B$ (1.0 T) at $T = 2$ K, one gets $\mu_{eff}(Co(1)) = 3.17\ \mu_B$, which is in reasonable agreement with the value 3.87 μ_B. Note that the theoretical estimate for two spin moments $S = 3/2$ in

the dimer $\mu_{eff}^{calc}(2\ K) = 5.47\ \mu_B$ even better agrees with the value 5.60 μ_B measured in a magnetic field of 0.5 T.

The magnetic field dependence of the magnetization $M(B)$ for complex **2** is shown in Fig. 7. The saturation magnetization is as high as 4 μ_B. The experimental dependence is not described by the Brillouin function for $S = 3/2 + 1/2$ (see Fig. 7, solid line). However, these data are consistent with the decrease in μ_{eff} for the Co(1) ion in high fields at 2 K. One can assume that in high fields (about 5 T) the Co(1) ion undergoes transition to the low-spin state ($S = 1/2$), whereas in weak fields ($B \le 0.5$ T) it remains in the high-spin state.

In the high-spin octahedral Co^{II} complexes with weak-field ligands, the central ion has the electronic configuration $d^7 = t_{2g}^5 e_g^2$, *i.e.*, the splitting in the ligand field (Δ) becomes smaller than the intra-atomic (Hund ferromagnetic) superexchange: $\Delta < P$. Indeed, the energy of stabilization of the high-spin state by the crystal field is $E^3 = -(5 \cdot 2/5 - 2 \cdot 3/5)\Delta = -4/5\Delta$, whereas for the low-spin state one has $E^1 = -(6 \cdot 2/5 - 1 \cdot 3/5)\Delta = -9/5\Delta$. Having denoted $E^3 - E^1 = \Delta$, one gets that at $\Delta < P$ the high-spin state ($S = 3/2$) is energetically more favorable. Octahedral symmetry leads to triple orbital degeneracy of the t_{2g}-level with the effective moment $l_{eff} = 1$. The degeneracy can be removed following the Jahn—Teller or the spin-orbital channel.[10] The spin-orbital coupling is of fundamental importance because it removes the degeneracy of the d_{xz}- and d_{yz}-levels and unfreezes the orbital moment. Distortion of the octahedron (stretching corresponds to $c/a > 1$, shrinkage corresponds to $c/a < 1$, where a and c are the experimental unit cell parameters) causes inversion of terms. Both mechanisms stabilize distorted configurations of the coordination site, the distortions being opposite in character. As a result, at $T > 60$ K the Co(1) ion is in the high-spin state with the orbital contribution $l = 1$ ($\mu_{eff}^{calc} = 6.48\ \mu_B$). At 60 K, "back distortion" of the octahedron occurs and the spin is now on the d_{xy}-orbital with $l = 0$ ($\mu_{eff}^{calc} = 5.47\ \mu_B$). Note that at $B = 5$ T one has $\mu_B H/\kappa \sim 3$ K, the intra-atomic exchange no longer provides an energy gain, and the Co(1) ion undergoes transition to the field-induced low-spin state.

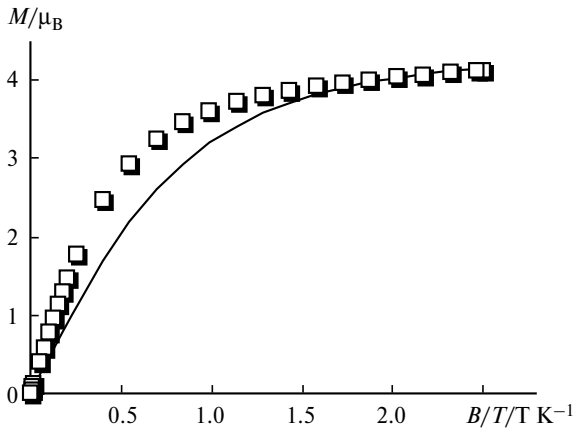

Fig. 7. Magnetic field dependence of the magnetization M of complex **2** at $T = 2$ K ($B/T = 2.5$ T K^{-1} corresponds to $B = 5$ T): open squares denote experimental data and the solid line is the Brillouin dependence for noninteracting spins $S = 1/2 + 3/2$ in the dimer.

Summing up, we have synthesized and structurally characterized the crystals of dinuclear complexes of Cu^{II} with 3-(3,5-dimethylpyrazol-1-yl)-6-(2-hydroxyethylamino)-1,2,4,5-tetrazine (**1**) and Co^{II} with 3-(3,5-dimethylpyrazol-1-yl)-6-(piperidin-1-yl)-1,2,4,5-tetrazine (**2**). Investigations of the magnetic (SQUID) and resonance (EPR) properties of complexes **1** and **2** showed that the nature of the nonmonotonic changes in the effective magnetic moment $\mu_{eff}(T)$ at $T < 60$ K is common to both structures. An increase and a decrease in μ_{eff} for **1** and **2**, respectively, is not related to exchange interactions, being due to the effect of spin-orbital coupling on the character of splitting of the t_{2g}- and e_g-levels in a nonequivalent central ion (Cu(1)/Cu(2), Co(1)). Structural distortions in the corresponding coordination sites are responsible for the admixture (**1**) or "freezing" (**2**) of the contribution of the magnetic orbital moment $l_{eff} = 1$. The irreversible character of the $\mu_{eff}(T)$ dependence near 60 K for polycrystalline samples of both compounds suggests that the character of structural distortions and, therefore, the total magnetic moment is related to the ligand structure.

Experimental

The synthesis of the starting 3,6-disubstituted tetrazines was reported earlier.[11]

IR spectra of solid samples (Nujol mulls) were recorded on a Perkin—Elmer Spectrum One Fourier IR spectrometer.

Elemental analysis was performed on automated CHN-analyzers (model EA 1108, Carlo Erba Instrument, Italy and Perkin—Emer Model PE 2400, Series II, USA) using a quantitative chemical analysis procedure according to GOST-R8.563.

Crystals of complexes for X-ray studies were grown from MeCN. Broken prismatic crystals were analyzed. X-ray diffraction experiments were carried out on an Xcalibur 3 automated X-ray diffractometer with a CCD detector (Mo-Kα radiation, graphite monochromator, 295(2) K, ω-scan). The absorption correction was introduced analytically using the polyhedron model. The structures were solved and refined by the full-matrix least squares method with respect to F^2 in the anisotropic approximation for non-hydrogen atoms using the SHELX program package.[12] Hydrogen atoms were located geometrically and included in the refinement in the isotropic approximation. Selected parameters of structural experiments are listed in Table 2 and the bond lengths and bond angles are listed in Table 1.

Magnetic measurements were carried out on a Quantum Design MPMS-5-XL SQUID magnetometer. The temperature dependences of the static magnetic susceptibilities $\chi(T)$ of the polycrystalline samples under study were measured at $B_0 = 0.5$ and 1.0 T in the temperature range 2—300 K. The magnetization curves $M(B)$ were obtained at 2 K in magnetic fields B ranging from 0 to 5 T. When constructing the dependence $\chi_{tot}(T) \cdot T$,

Table 2. Selected parameters of X-ray experiments for complexes **1** and **2**

Parameter	**1**	**2**
Crystal size/mm^3	0.24×0.13×0.06	0.17×0.11×0.03
Temperature/K	295(2)	295(2)
Crystal system	Monoclinic	Orthorhombic
Molecular formula	$C_{18}H_{26}Cl_4Cu_2N_{14}O_2$	$C_{24}H_{34}Cl_4Co_2N_{14}$
Space group	$P2_1/c$	$P2_12_12$
a/Å	9.9102(13)	11.3924(11)
b/Å	14.518(2)	15.7769(15)
c/Å	10.0251(10)	9.0804(4)
α/deg	90	90
β/deg	90.440(9)	90
γ/deg	90	90
d_{calc}/g cm^{-3}	1.703	1.584
μ/mm^{-1}	1.891	1.385
V/Å^3	1442.3(3)	1632.1(2)
Z	2	2
Number of independent reflections	3488	3621
R_{int}	0.0675	0.0244
Completeness (%)	97.6	99.2
θ/deg	26.00	28.28
Goodness of Fit, GOOF	1.000	0.999
Final R-factors [$I > 2\sigma(I)$]		
R_1	0.0523	0.0333
wR_2	0.1277	0.0678
Residual electron density /e·Å^{-3}, ρ_{max}/ρ_{min}	0.589/−0.666	0.395/−0.345

it was assumed that the diamagnetic response of the organic framework contributes linearly to the overall SQUID signal. This response was measured in the entire temperature interval and then subtracted from the overall SQUID signal.

EPR measurements were carried out on a conventional ERS-231 homodyne c.w. EPR spectrometer (X-band, ~9.3 GHz) using a rectangular TE_{102} cavity. The EPR spectra were recorded in the temperature range 93—350 K (microwave power about 2 mW). The temperature was set and stabilized at a rate of 1—2 K min^{-1} and an accuracy of 0.1 K using a flow nitrogen cryostat.

The spin contribution to the magnetic susceptibility was evaluated using a double integration (the Schumacher—Slichter method) of an EPR signal with allowance for the field sweep condition $\delta B_{sw} > 5\Delta B$ (ΔB is the peak-to-peak EPR line width). In this case, for a Lorentzian EPR signal one gets an error of about 10%. As a reference, carbon pyrolysate with $g = 2.00283$ was used.

Synthesis of complexes 1 and 2 (general procedure). To a solution of tetrazine (0.1 mmol) in acetonitrile (10 mL), a solution of the metal salt (0.1 mmol) in acetonitrile (10 mL) was added. The reaction mixture was heated for 1 h under reflux with continuous magnetic stirring. The solution was concentrated to 2/3 of its initial volume and the solvent was slowly evaporated at about 20 °C. The residues were filtered off and recrystallized from acetonitrile.

Complex **1**. The yield was 70%. Dark cherry crystals, m.p. >350 °C (from MeCN). Found (%): C, 29.30; H, 3.49; N, 26.49. $C_{18}H_{26}Cl_4Cu_2N_{14}O_2$. Calculated (%): C, 29.24; H, 3.54; N, 26.52. IR, ν/cm^{-1}: 3486, 1583, 1501, 1470, 1457, 1435, 1059, 1037, 1016.

Complex **2**. The yield was 75%. Dark green crystals, m.p. >350 °C (from MeCN). Found (%): C, 37.17; H, 4.19; N, 25.52. $C_{18}H_{26}Cl_4Co_2N_{14}O_2$. Calculated (%): C, 37.03; H, 4.40; N, 25.20. IR, ν/cm^{-1}: 1567, 1495, 1453, 1407, 1094, 1035, 1008, 983.

X-ray data were deposited at the Cambridge Structural Database. They are free of charge and available from deposit@ccdc.cam.ac.uk on request.

This work was financially supported by the Russian Foundation for Basic Research (Project Nos 05-03-32094-a, 07-03-96112-r_ural_a, and 07-03-96113-r_ural_a), the Presidium of the Russian Academy of Sciences (Project No. 26), the Siberian and Ural Branches of the Russian Academy of Sciences (interdisciplinary program, Integration Project No. 37), the Council on Grants at the President of the Russian Federation (Program of State Support of Leading Scientific Schools, Grant NSh-3758.2008.3).

References

1. V. I. Ovcharenko, R. Z. Sagdeev, *Usp. Khim.*, 1999, **68**, 381 [*Russ. Chem. Rev.* (*Egnl. Transl.*), 1999, **68**].
2. W. Kaim, *Coord. Chem. Rev.*, 2002, **230**, 127.
3. S. Patra, Th. A Miller, B. Sarkar, M. Niemeyer, M. D. Ward, G. Kumar, *Inorg. Chem.*, 2003, **42**, 4707.
4. A. E. Malkov, I. G. Fomina, A. A. Sidorov, G. G. Aleksandrov, I. M. Egorov, N. I. Latosh, O. N. Chupakhin, G. L. Rusinov, Yu. V. Rakitin, V. M. Novotortsev, V. N. Ikorskii, I. L. Eremenko, I. I. Moiseev, *J. Mol. Struct.*, 2003, **656**, 207.
5. M. A. Kiskin, A. A. Sidorov, I. G. Fomina, G. L. Rusinov, R. I. Ishmetova, G. G. Aleksandrov, Yu. G. Shvedenkov, Zh. V. Dobrokhotova, V. M. Novotortsev, O. N. Chupakhin, I. L. Eremenko, I. I. Moiseev, *Inorg. Chem. Commun.*, 2005, **8**, 524.
6. E. V. Cherdantseva, R. I. Ishmetova, N. I. Latosh, O. V. Koryakova, G. L. Rusinov, *Sb. dokl. Mezhdunar. konf. "Tekhnicheskaya khimiya: ot teorii k praktike"* [*Proc. Int. Conf. "Technical Chemistry: from Theory to Practice"*] (*Perm´, Russia, September 8—12, 2008*), Perm´, 2008, 410 (in Russian).
7. Z. Ropka, R. J. Radwanski, *Phys. Rev.*, 2003, **67**, 172401.
8. A. Podlesnyak, S. Streule, J. Mesot, M. Medarde, E. Pomjakushina, K. Conder, A. Tanaka, M. W. Haverkort, D. I. Khomskii, *Phys. Rev. Lett.*, 2006, **97**, 247208.
9. C. Oliva, L. Forni, A. D. Ambrosio, F. Novarrini, A. D. Stepanov, Z. D. Kagramanov, A. I. Mikhailichenko, *Appl. Catal. A*, 2001, **1—2**, 245.
10. K. I. Kugel, D. I. Khomskii, *Usp. Fiz. Nauk*, 1982, **136**, 621 [*Sov. Phys.-Usp.* (*Engl. Transl.*), 1982, **136**].
11. N. I. Latosh, G. L. Rusinov, I. N. Ganebnykh, O. N. Chupakhin, *Zh. Organ. Khim.*, 1999, **35**, 1392 [*Russ. J. Org. Chem.* (*Engl. Transl.*), 1999, **35**].
12. G. M. Sheldrick, *SHELXL97*, *SHELXS97*, *Program for the Refinement of Crystal Structure*, Göttingen University, Göttingen, Germany, 1997.

Received June 11, 2009;
in revised form October 21, 2009